

New C-5 substituted pyrrolotriazine dual inhibitors of EGFR and HER2 protein tyrosine kinases

Harold Mastalerz,^{a,*} Ming Chang,^b Ping Chen,^b Pierre Dextraze,^c Brian E. Fink,^b Ashvinikumar Gavai,^b Bindu Goyal,^b Wen-Ching Han,^b Walter Johnson,^a David Langley,^a Francis Y. Lee,^b Punit Marathe,^b Arvind Mathur,^b Simone Oppenheimer,^b Edward Ruediger,^c James Tarrant,^a John S. Tokarski,^b Gregory D. Vite,^b Dolatrai M. Vyas,^a Henry Wong,^a Tai W. Wong,^b Hongjian Zhang^b and Guifen Zhang^a

^a*Departments of Oncology Chemistry, Discovery Biology, Pharmaceutical Candidate Optimization, Computer Aided Drug Design, and Chemical Synthesis, 5 Research Parkway, Wallingford, CT 06492-1951, USA*

^b*Bristol-Myers Squibb Pharmaceutical Research Institute, PO Box 4000, Princeton, NJ 08543-4000, USA*

^c*100 Boul. de l'Industrie, Candiac, Que., Canada J5R 1J1*

Received 29 November 2006; revised 19 December 2006; accepted 5 January 2007

Available online 12 January 2007

Abstract—Novel C-5 substituted pyrrolotriazines were optimized for dual EGFR and HER2 protein tyrosine kinase inhibition. The lead compound exhibited promising oral efficacy in both EGFR and HER2 driven human tumor xenograft models. It is hypothesized that its C-5 morpholine side chain binds in the ribose phosphate portion of the ATP binding pocket.

© 2007 Elsevier Ltd. All rights reserved.

The epidermal growth factor receptor (EGFR, ErbB1 or HER1) and the human epidermal growth factor receptor 2 (HER2, ErbB2) are members of the ErbB family of receptor tyrosine kinases and have been clinically validated as targets for cancer therapy.¹ Their frequent co-expression in a variety of tumor types and their capacity to form heterodimers with other members of the ErbB family provide a strong rationale for simultaneously tar-

geting both of these receptors.² There are currently several small molecule, ATP-competitive, reversible, dual EGFR, and HER2 kinase inhibitors in clinical development. These include: lapatinib (GW572016),³ AEE-788,⁴ and BMS-599626 (**1**).⁵ The latter utilizes the bicyclic pyrrolo[2,1-f][1,2,4]triazine ring system as a scaffold for the construction of an ATP mimic.⁶ Its lipophilic C-4 substituent provides potent and selective kinase inhibition,

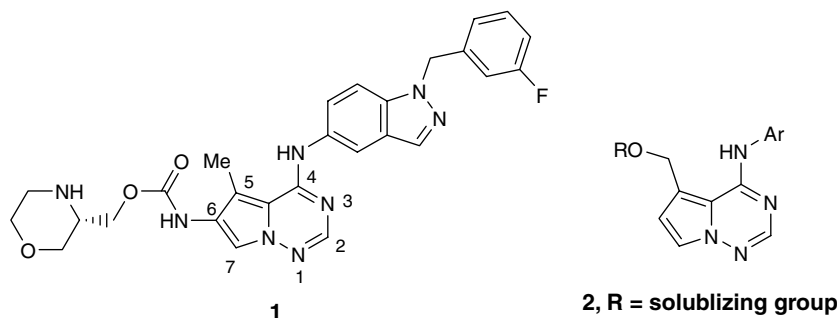


Figure 1. Pyrrolotriazine dual EGFR and HER2 kinase inhibitors.

Keywords: EGFR; HER2; Receptor tyrosine kinase inhibitor; Pyrrolotriazine.

* Corresponding author. Tel.: +1 203 677 7773; e-mail: harold.mastalerz@bms.com

while its C-6 solubilizing side chain imparts good pharmacokinetics and further potency. We explored the SAR of analogs of **1** (Fig. 1) where the solubilizing group is tethered to C-5 via a methylene ether linkage, that is **2**, and describe our results in this report.

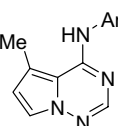
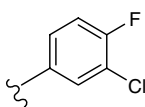
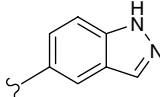
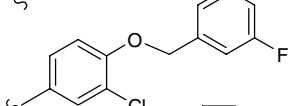
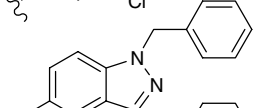
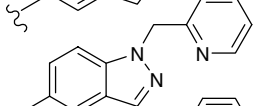
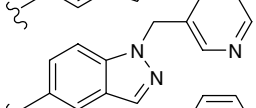
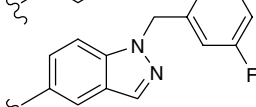
5-Methyl-pyrrolotriazines with different C-4 substituents (compounds **4–10** in Table 1) were prepared by reaction of 4-chloro-5-methyl-pyrrolotriazine **3**⁶ with anilines in the presence of a base (Scheme 1). To prepare C-5 methylene ether analogs (compounds **12–27** in Table 2), the 5-methyl group of **3** was first brominated to give **11**.⁷ This was treated with an excess of the alcohol of interest followed by 1-(3-fluorobenzyl)-1*H*-indazol-5-amine to give the ether analogs. A more efficient procedure was used with alcohols of limited availability. For this, **11** was converted into alcohol **28** by solvolysis in aqueous acetonitrile followed by reaction with 1-(3-fluorobenzyl)-1*H*-indazol-5-amine. Treatment of **28** with thionyl chloride gave a relatively unstable 5-chloromethyl intermediate, **29**, that was reacted with a slight excess of the alcohol of interest to give the corresponding ether analog.

The C-4 analogs of **24** (compounds **32–38** in Table 3) were prepared by first converting **3** to the 4-methyl-

sulfide, **30** (Scheme 2). Bromination of the 5-methyl group followed by reaction with (*S*)-*tert*-butyl 2-(hydroxymethyl)morpholine-4-carboxylate⁸ gave ether intermediate **31**. Oxidation of the sulfide group followed by reaction with different anilines and then deprotection gave the C-4 analogs.

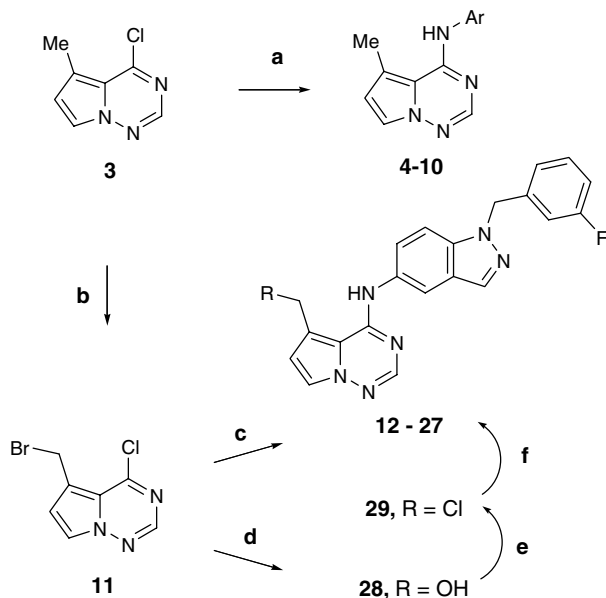
Analogs **35–38** (Table 3) have chiral phenylethyl groups attached to N-1 of the indazole residue. To prepare the aminoindazole that was used to make **35**, nitroindazole **39** was coupled with (*S*)-1-phenylethanol using a Mitsunobu reaction (Scheme 3).⁹ This gave a 2:1 mixture of the desired N-1 alkylation product, **40**, and its N-2 regioisomer. The isomers were separated by chromatography and their regiochemistry was established by 2D NMR (COSY). Reduction of the nitro group gave the aminoindazole, **41**, that was used to make **35** as outlined above. Analog **36** was similarly prepared from (*R*)-1-phenylethanol. Chiral HPLC analysis of **35** and **36** indicated that they were homochiral and that the Mitsunobu reaction had proceeded with complete inversion of configuration (ee > 99%). Their *m*-fluoro analogs, **37** and **38**, were similarly prepared as a racemic mixture from 1-(3-fluorophenyl)ethanol. They were separated by preparative chiral HPLC and their configuration was

Table 1. Structure–activity relationship for the C-4 position

			
Compound	Ar	HER2 ^{a,b} IC ₅₀ (μM)	EGFR ^b IC ₅₀ (μM)
4		>1	0.10
5		>1	0.21
6		0.43	0.25
7		0.11	0.086
8		0.31	0.20
9		0.25	1.8
10		0.088	0.081

^a Recombinant HER2 cytoplasmic sequence is expressed in Sf9 insect cells as an untagged protein and purified by ion-exchange chromatography. HER2 kinase activity is measured under the same conditions as for EGFR. See Refs. 5 and 6 for assay conditions.

^b IC₅₀ values are reported as means of at least three determinations. Variability around the mean value was <15%.



Scheme 1. Reagents and conditions: (a) ArNH_2 (1.0 equiv), NaHCO_3 (2 equiv), CH_3CN , rt; (b) NBS (1.05 equiv), benzoyl peroxide (catalytic), CCl_4 , N_2 , reflux, 1 h (74%); (c) ROH (10 equiv), CH_3CN , NaHCO_3 (2 equiv), rt and then 1-(3-fluorobenzyl)-1*H*-indazol-5-amine (0.9 equiv), NaHCO_3 (2 equiv), CH_3CN , rt and then deprotection (33% TFA, CH_2Cl_2 , rt) if required; (d) NaHCO_3 (2.5 equiv), $\text{CH}_3\text{CN}/\text{H}_2\text{O} = 10:1$, rt, 3 days, then 1-(3-fluorobenzyl)-1*H*-indazol-5-amine (0.9 equiv), NaHCO_3 (0.8 equiv), rt, 18 h (65%); (e) SOCl_2 (1.1 equiv), CH_2Cl_2 , rt; (f) ROH (1.5 equiv), DIPEA (1.1 equiv), CH_2Cl_2 , rt, 3 days and then deprotection (33% TFA, CH_2Cl_2 , rt) if required.

assigned according to their biochemical potency relative to that of the des-fluoro analogs, **35** and **36**.

The 6-methoxy analog of **24** (compound **45**, Table 3) was prepared from 5-methyl ester **42**¹⁰ as outlined in Scheme 4. The ester was reduced to alcohol **43** which was then converted to acetate **44**. Heating **44** with an excess of (*S*)-*tert*-butyl 2-(hydroxymethyl)morpholine-4-carboxylate followed by deprotection gave **45**.

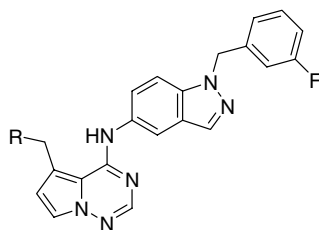
The SAR of 5-methyl-pyrrolotriazines with different C-4 substituents (Table 1) was found to parallel that reported for 5,6-disubstituted pyrrolotriazines.¹¹ Analogs with small C-4 anilines or bicyclic heterocycles (compounds **4** and **5**) were selective EGFR inhibitors. Appending a lipophilic benzyl group to the C-4 aniline increased HER2 kinase inhibition without reducing EGFR inhibition (compounds **6** and **7**). The 2-picolyloxy analog, **8**, showed a slight drop in overall potency, while its 3-picolyloxy isomer, **9**, was a HER2 selective inhibitor. The *m*-fluorobenzylindazolylamino side chain of **10** was found to provide the best dual EGFR and HER2 kinase inhibition and was therefore kept as the C-4 substituent for the SAR study of different C-5 methylene ether solubilizing groups.

Promising C-5 analogs were screened for their antiproliferative activity against the N87 cell line. This is a human gastric carcinoma that overexpresses both EGFR and HER2.^{5,12} Analogs were also screened in HT29 (human colon carcinoma) or A2780 (human ovarian carci-

noma) cell proliferation assays. These are cell lines that do not depend on EGFR or HER2 signaling and provide a check for off-target antiproliferative effects. The 5-hydroxymethyl derivative, **28**, and its ether analogs, **12** and **13**, were less potent kinase inhibitors than the 5-methyl compound, **10** (Table 2). Acid **14** showed good kinase inhibition and modeling suggested that the acid group could either interact with the conserved Lys745 normally involved in binding the phosphate group of ATP or Cys773 of the solvent-exposed hinge region (see Fig. 2A for the position of Cys773). It did not show antiproliferative activity, presumably because of poor cell permeability. The neutral ester and amide analogs, **15** and **16**, were less potent kinase inhibitors. Analogs with acyclic basic amino groups (compounds **17–19**) showed better potency in both the kinase and cell assays. The best of these was **18** which had a propylene spacer between the amino and ether groups. It was more potent than its *N,N*-dimethyl analog, **20**, and also showed good stability when incubated with mouse liver microsomes. The latter observation was found to be general; pyrrolotriazine analogs with basic primary or secondary amine substituents showed better microsomal stability than their tertiary or *N*-acylated counterparts. This has been seen with other chemotypes and it has been suggested that the greater polarity and basicity of the primary or secondary amines reduces their rate of metabolism by the CYP3A4 isozyme.¹³ The piperidine ether, **21**, showed similar kinase and antiproliferative activity, while homolog **22** and its 3-piperidyl isomer, **23**, were less potent. Morpholine analog **24** showed good kinase inhibition and significantly enhanced antiproliferative activity. The latter appears to be due to EGFR and HER2 kinase inhibition since **24** did not show significant activity against the A2780 cell line. Its improved cellular potency relative to analogs like **18** may be the result of better cell permeability with the less basic morpholine side chain.¹⁴ Its *R*-enantiomer, **25**, showed a similar profile and modeling suggested that the morpholine group of both enantiomers can make similar hydrogen bond contacts in the ribose-phosphate portion of the ATP binding pocket (see below). Transposed analog **26** and racemic oxazepine **27** were less potent.

The SAR of the C-4 substituent of **24** was then examined to see if further improvements were possible (Table 3). Benzyl ether **32** and picolyloxy analogs, **33** and **34**, were found to be less potent. The *R*-(1-phenylethyl) analog, **35**, was more potent than its enantiomer, **36**, suggesting that its C-4 substituent experiences a better fit in the hydrophobic specificity pocket. The corresponding fluoro derivatives, **37** and **38**, were more potent with the former showing a profile similar to that of **24**. Finally, methoxy analog **45** was prepared to gauge the effect of substitution at C-6. The observed drop in potency indicated that this was not tolerated.

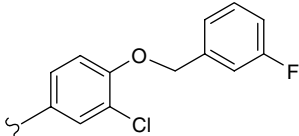
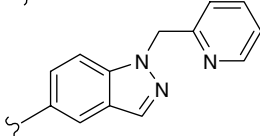
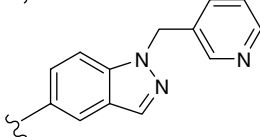
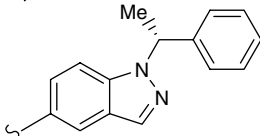
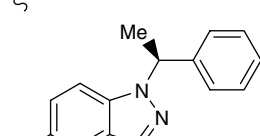
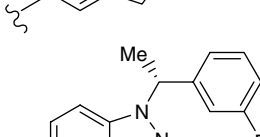
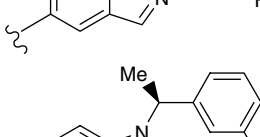
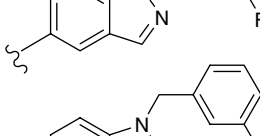
Potential binding modes for compound **24** in the ATP binding site were modeled after the published X-ray structure of the complex between lapatinib and the EGFR.¹⁵ Two binding modes were considered possible and these are shown in Figure 2. In both cases, the pyrrolotriazine core is oriented in the ATP binding site such

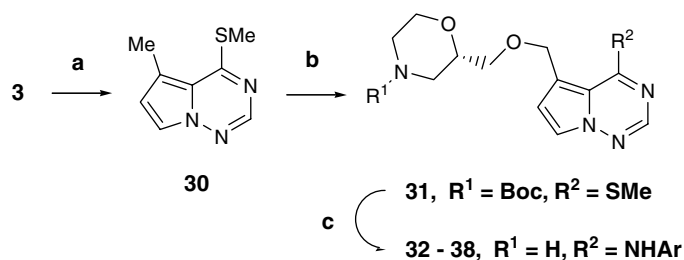
Table 2. Structure–activity relationship for the C-5 position

Compound	R	IC ₅₀ ^a (μM)				Metabolic stability ^e
		HER2	EGFR	N87 ^b	HT29 ^c or A2780 ^d	
10	H	0.088	0.081	0.38	>10 ^c	0.14
28	HO	0.11	0.12	7.4	>10 ^c	nd
12	MeO	0.42	0.34	nd	nd	0.24
13		0.42	0.49	nd	nd	nd
14		0.018	0.030	>10	>10 ^d	nd
15		0.28	0.46	1.7	nd	nd
16		0.11	0.14	1.7	>10 ^d	nd
17		0.09	0.09	1.7	8.3 ^d	nd
18		0.06	0.064	0.64	7.4 ^d	0.01
19		0.13	0.16	nd	nd	nd
20		0.56	0.62	nd	nd	0.12
21		0.07	0.073	0.33	6.0 ^d	0.02
22		0.12	0.13	0.72	4.9 ^d	nd
23		0.17	0.19	0.98	7.4 ^d	nd
24		0.055	0.061	0.083	8.7 ^d	0.07
25		0.060	0.083	0.13	>10 ^d	nd
26		0.59	0.64	3.0	>10 ^d	nd
27		0.14	0.21	2.0	>10 ^d	nd

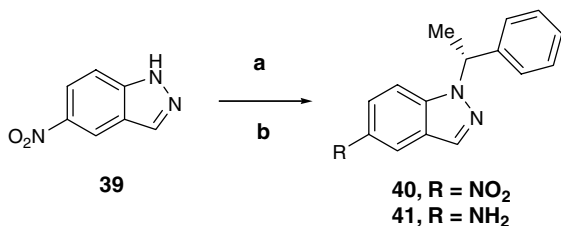
^a IC₅₀ values are reported as means of at least three determinations. Variability around the mean value was <15%.^b Cell line N87 is a human gastric carcinoma that overexpresses both EGFR and HER2.⁵^{c,d} Cell lines HT29 (human colon carcinoma) and A2780 (human ovarian carcinoma) do not depend on EGFR or HER2 signaling.⁵^e Rate of metabolism (nmol min⁻¹ mg protein⁻¹) by mouse liver microsomes after a 10-min incubation at 3 μM in the presence of NADPH.

Table 3. Structure–activity relationship for the C-4 position of **24**

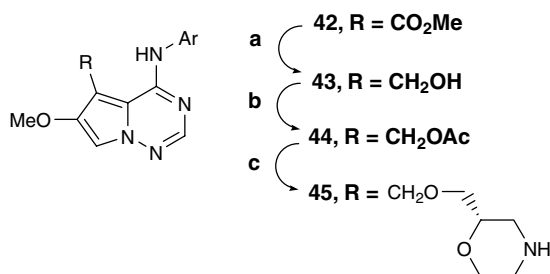
Compound	Ar	IC ₅₀ ^a (μM)		
		HER2	EGFR	N87
32		0.56	0.57	0.61
33		0.38	0.50	0.24
34		0.41	0.81	0.55
35		0.13	0.12	0.66
36		0.85	0.69	2.2
37		0.041	0.068	0.13
38		0.51	0.40	nd
45^b		0.25	0.43	3.4

^a IC₅₀ values are reported as means of at least three determinations. Variability around the mean value was <15%.^b Compound **45** is the 6-methoxy analog of **24**.

Scheme 2. Reagents and conditions: (a) NaSMe (1.5 equiv), THF, rt; (b) NBS (1.05 equiv), benzoyl peroxide (catalytic), CCl₄, N₂, reflux, 10 min, then (*S*)-*tert*-butyl 2-(hydroxymethyl)morpholine-4-carboxylate (1.5 equiv), toluene, reflux, 55%; (c) *m*-CPBA (2.1 equiv), CH₂Cl₂, 0 °C to rt, 30 min, then ArNH₂ (1.0 equiv), rt, then 15% TFA/CH₂Cl₂.



Scheme 3. Reagents and condition: (a) (S)-(+)-1-phenylethanol (2.0 equiv), 1,1'-azobis(N,N-dimethyl formamide) (2.0 equiv) PBU_3 (2.0 equiv), toluene, 80 °C, 64%; (b) H_2 (1 atm), catalytic $\text{Pd}(\text{OH})_2/\text{C}$, MeOH, 81%.



Scheme 4. Reagents and conditions: (a) LiAlH_4 (5 equiv), THF, 0 °C to rt, 68%; (b) AcCl (1.2 equiv), DIPEA (1.5 equiv) DCM, 0 °C, 75%; (c) (S)-tert-butyl 2-(hydroxymethyl)morpholine-4-carboxylate (20 equiv), DCE, 85 °C, 18 h then 50% TFA, DCE, 24%.

that there is a hydrogen bond between N-1 and the hinge region Met769 NH and the C-4 benzyl indazole group extends back into a deep hydrophobic pocket formed partially by the C-helix. The C-5 substituent can either extend out toward the solvent (Fig. 2A) or into the ribose phosphate pocket (Fig. 2B). In the former model the protonated morpholine NH can hydrogen bond with the side chains of Cys773 and Asp776. In the latter, the protonated morpholine NH can hydrogen bond with the side chains of Asp831 and Asn818, and also with the backbone carbonyl oxygen of Arg817. Also in this model there exists an intramolecular hydrogen bond between the C4 aniline NH and the C5 ether oxygen. The docked poses were energy-minimized in Maestro¹⁶ using

the OPLS-AA force field¹⁷ and the GBSA continuum model,¹⁸ an implicit solvation model. The resultant energy calculations (not shown) favor the latter model. The C-5 side chains of quinazoline EGFR and HER2 kinase inhibitors have recently been hypothesized to similarly extend into the ribose portion of the ATP binding pocket.¹⁹

The preliminary data for **24** showed promise and therefore it underwent further evaluation. It exhibited good selectivity in a small panel of kinases (Table 4) and a dose-dependent inhibition of HER2 protein phosphorylation in N87 cells (Fig. 3) that was consistent with the cell proliferation assay data.

Table 4. Kinase selectivity profile for **24**

Kinase	IC_{50}^a (μM)
EGFR	0.061
HER2	0.055
Met	6.5
LCK	>5
VEGFR2	>10
CDK2	>50
p38	>50
PKA	>50

^a IC_{50} values are reported as means of at least three determinations. Variability around the mean value was <15%.

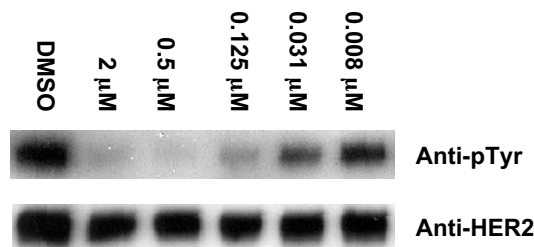


Figure 3. Compound **24** inhibits receptor phosphorylation in N87 Cells. These were treated with compound **24** for 1 h at the concentration indicated and cell lysates were analyzed by Western blotting with anti-phosphotyrosine and anti-HER2 antibodies.

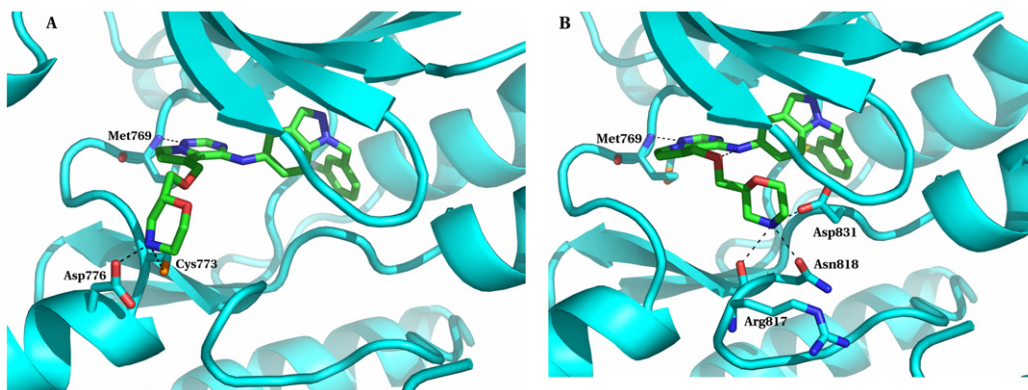


Figure 2. Predicted binding modes of compound **24** modeled in the X-ray structure of the lapatinib/EGFR kinase complex¹⁵. In part A of the figure the C-5 side chain extends out toward the solvent where the protonated morpholine NH hydrogen bonds with Cys773 and Asp776. In part B of the figure the C-5 side chain extends into the ribose phosphate binding region where the protonated morpholine NH hydrogen bonds with the Asp831, Asn818, and Arg817. Image created with Pymol from DeLano Scientific LLC, San Carlos, CA, USA. <http://www.pymol.org>.

Table 5. In vivo antitumor activity of **24** against GEO and N87 xenografts implanted subcutaneously in athymic mice

Tumor model	Dose ^a (mg kg ⁻¹)	Schedule	% TGI ^b	P ^c
N87	30	QD × 21	28	0.3329
	60		51	0.0037
	120		70	0.0001
	240		111	0.0001
GEO	30	QD × 14	21	0.3329
	60		55	0.0528
	120		71	0.0037
	240		91	0.0037

^a Vehicle: propylene glycol/water (50:50).^b Percent tumor growth inhibition during treatment. Tumor cells were implanted subcutaneously in athymic mice and staged to approximately 100 mg prior to the initiation of drug therapy. Activity is defined as %TGI ≥ 50%.^c Probability for median tumor weight at the end of drug treatment.

Compound **24** showed acceptable permeability in the Caco-2 bilayer model ($P_c = 64$ nm/s) suggesting that good oral absorption may be achieved in vivo. The free fraction (f_u) of the compound in mouse serum was 2.6% as determined by equilibrium dialysis at 10 μ M. It was administered orally (50 mg kg⁻¹ dose) to male Balb/C mice and showed a 4 h AUC of 29 μ M h and a 4 h plasma concentration of 5.8 μ M. This was about 70-fold higher than its antiproliferative IC₅₀ versus the N87 cell line in vitro and therefore it was evaluated in vivo in the N87 human gastric carcinoma (HER2 and EGFR driven) and the GEO human colon carcinoma (EGFR driven) xenograft models. Orally administered **24** was found to be well tolerated in both studies; treated animals exhibited no clinically observable sign of toxicity or weight loss at the highest test dose of 240 mg/kg. It elicited robust and dose-proportional tumor responses over the dose range of 60–240 mpk in both tumor models (Table 5).²⁰

In summary, it was found that pyrrolotriazines with a basic solubilizing group that is tethered to C-5 via a methylene ether linkage can show potent, selective inhibition of both the EGFR and the HER2 kinases. Modeling studies suggest that the C-5 solubilizing group may extend into the ribose-phosphate binding region of the ATP binding pocket where it can participate in multiple hydrogen bonding interactions. The lead compound, **24**, exhibited good kinase selectivity, antiproliferative potency, oral exposure, and efficacy in tumor xenograft models. This effort was followed by a broader examination of C-5 solubilizing groups and the results will be described in the future.

References and notes

- (a) Baselga, J.; Arteaga, C. L. *J. Clin. Oncol.* **2005**, *23*, 2445; (b) Kamath, S.; Buolamwini, J. K. *Med. Res. Rev.* **2006**, *26*, 569, and references therein.
- Baselga, J. *Ann. Oncol.* **2002**, *13*, 8.
- (a) Rusnak, D. W.; Lackey, K.; Affleck, K.; Wood, E. R.; Alligood, K. J.; Rhodes, N.; Kieth, B. R.; Murray, K. G.; Knight, W. B.; Mullin, R. J.; Gilmer, T. M. *Mol. Cancer Ther.* **2001**, *1*, 85; (b) Burris, H. A. *The Oncologist* **2004**, *9*(Suppl. 3), 10.
- Traxler, P.; Allegrini, P. R.; Brandt, R.; Bruegggen, J.; Cozens, R.; Fabbro, D.; Grosios, K.; Lane, H. A.; McSheehy, P. L.; Mestan, J.; Meyer, T.; Tang, C.; Wartmann, M.; Wood, J.; Caravatti, G. *Cancer Res.* **2004**, *64*, 4931.
- Wong, T. W.; Lee, F. Y.; Yu, C.; Luo, F. R.; Oppenheimer, S.; Zhang, H.; Smykla, R. A.; Mastalerz, H.; Fink, B. E.; Hunt, J. T.; Gavai, A. V.; Vite, G. D. *Clin. Cancer Res.* **2006**, *12*, 6186.
- Hunt, J. T.; Mitt, T.; Borzilleri, R.; Gullo-Brown, J.; Fargnoli, J.; Fink, B.; Han, W.-C.; Mortillo, S.; Vite, G.; Wautlet, B.; Wong, T.; Yu, C.; Zheng, X.; Bhide, R. *J. Med. Chem.* **2004**, *47*, 4054.
- For experimental procedures, see: Mastalerz, H.; Zhang, G.; Tarrant, J.; Vite, G. D. US 6,908,916.
- Brenner, E.; Baldwin, R. M.; Tamagnan, G. *Org. Lett.* **2005**, *7*, 937.
- (a) Fernandez, P. A.; Bellamy, T.; King, M.; Madge, D. J.; Selwood, D. L. *Heterocycles* **2001**, *55*, 1813; (b) Tsunoda, T.; Yamamiya, Y.; Ito, S. *Tetrahedron Lett.* **1993**, *34*, 1639.
- Mastalerz, H.; Gavai, A. V.; Fink, B.; Struzynski, C.; Tarrant, J.; Vite, G. D.; Wong, T. W.; Zhang, G.; Vyas, D. M. *Can. J. Chem.* **2006**, *84*, 528.
- Fink, B. E.; Vite, G. D.; Mastalerz, H.; Kadow, J. F.; Kim, S.-H.; Leavitt, K. J.; Du, K.; Crews, D.; Mitt, T.; Wong, T. W.; Hunt, J. T.; Vyas, D. M.; Tokarski, J. S. *Bioorg. Med. Chem. Lett.* **2005**, *15*, 4774.
- Additional cell proliferation data (not shown) using the HER2 overexpressing BT-474 human breast tumor cell line and a constitutively activated Sal2 murine salivary gland tumor that expresses a CD8HER2 fusion protein were found to track with these observed for the N87 cell line.
- (a) Smith, A. S.; van de Waterbeemd, H. In *Pharmacokinetics and Metabolism in Drug Design*; Wiley-VCH: Weinheim, 2001; p 84; (b) Smith, D. A.; Jones, C. J.; Walker, D. K. *Med. Res. Rev.* **1996**, *16*, 243.
- Based on pK_a 's (H₂O) of 8.3 for morpholine versus 10.2 for 1-amino-3-hydroxypropane from: Perrin, D.D. *Dissociation Constants of Organic Bases in Aqueous Solution. Supplement 1972*; Butterworths: London, UK, 1972.
- Wood, E. R.; Truesdale, A. T.; McDonald, O. B.; Yuan, D.; Hassell, A.; Dickerson, S. H.; Ellis, B.; Pennisi, C.; Horne, E.; Lackey, K.; Alligood, K. J.; Rusnak, D. W.; Gilmer, T. M.; Shewchuk, L. *Cancer Res.* **2004**, *64*, 6652.
- Schrodinger, L.L.C. 2003. 32nd Floor, Tower 45, 120 West Forty-Fifth Street, New York, 10036.
- Kaminski, G. A.; Friesner, R. A.; Tirado-Rives, J.; Jorgensen, W. L. *J. Phys. Chem. B* **2001**, *105*, 6474.
- Yu, Z.; Jacobson, M. P.; Friesner, R. A. *J. Comput. Chem.* **2006**, *27*, 72.
- (a) Ballard, P.; Bradbury, R. H.; Harris, C. S.; Hennequin, L. F. A.; Dickinson, M.; Johnson, P. D.; Kettle, J. G.; Kinowska, T.; Leach, A. G.; Morgentin, R.; Pass, M.; Ogilvie, D. J.; Olivier, A.; Warin, N.; Williams, E. J. *Bioorg. Med. Chem. Lett.* **2006**, *16*, 1633; (b) Ballard, P.; Bradbury, C. S.; Hennequin, L. F. A.; Dickinson, M.; Johnson, P. D.; Kettle, J. G.; Kinowska, T.; Morgentin, R.; Ogilvie, D. J.; Olivier, A. *Bioorg. Med. Chem. Lett.* **2005**, *15*, 4226.
- For experimental details, see Ref. 5.